

## Investigation of the microstructure, mechanical properties and thermal stability of nanocomposite coatings based on amorphous carbon

A. V. Andreev, I. Y. Litovchenko, A. D. Korotaev, and D. P. Borisov

Citation: [AIP Conference Proceedings](#) **1683**, 020008 (2015); doi: 10.1063/1.4932698

View online: <http://dx.doi.org/10.1063/1.4932698>

View Table of Contents: <http://scitation.aip.org/content/aip/proceeding/aipcp/1683?ver=pdfcov>

Published by the [AIP Publishing](#)

---

### Articles you may be interested in

[Features of structure-phase state of multielement nanocomposite coatings based on amorphous carbon](#)  
AIP Conf. Proc. **1623**, 11 (2014); 10.1063/1.4898870

[Microstructural and mechanical properties of thermal barrier coating at 1400°C treatment](#)  
Theor. Appl. Mech. Lett. **4**, 021008 (2014); 10.1063/2.1402108

[Study of Microstructure, Tribological, Thermal and Mechanical Properties of Ultrahigh Molecular Weight Polyethylene \(UHMWPE\)/Copper Nanocomposite](#)  
AIP Conf. Proc. **1276**, 260 (2010); 10.1063/1.3504307

[Microstructure and mechanical properties of nanocomposite amorphous carbon films](#)  
J. Vac. Sci. Technol. A **20**, 1390 (2002); 10.1116/1.1486227

[Thermal stability and electrical properties of hydrogenated amorphous carbon film](#)  
Appl. Phys. Lett. **65**, 3200 (1994); 10.1063/1.112440

---

# Investigation of the Microstructure, Mechanical Properties and Thermal Stability of Nanocomposite Coatings Based on Amorphous Carbon

A. V. Andreev<sup>1, a)</sup>, I. Y. Litovchenko<sup>2, 3, b)</sup>, A. D. Korotaev<sup>1, 2, 3, c)</sup>,  
and D. P. Borisov<sup>1, 3, d)</sup>

<sup>1</sup> National Research Tomsk State University, Tomsk, 634050 Russia

<sup>2</sup> Siberian Physical-Technical Institute, Tomsk, 634050 Russia

<sup>3</sup> Institute of Strength Physics and Materials Science SB RAS, Tomsk, 634055 Russia

<sup>a)</sup> Corresponding author: alexardas@mail.ru

<sup>b)</sup> litovchenko@spti.tsu.ru

<sup>c)</sup> korotaev@phys.tsu.ru

<sup>d)</sup> borengin@mail.ru

**Abstract.** The Ti-C-Ni-Cr and Ti-C-Ni-Cr-Al-Si nanocomposite coatings based on amorphous carbon and the nanosized particles were synthesized by magnetron method. The results of the microstructure features and mechanical properties investigations of these coatings are presented. The thermal stability of microstructure and properties of these coatings at tempering up to 900°C were investigated. These coatings have a high (11–18 GPa) hardness, low ( $\mu < 0.2$ ) the coefficient of friction and high thermal stability of the microstructure and properties up to 700°C. The features of elastically stressed state of nanosized particles in these coatings were founded. A high local internal stresses in the TiC nanoscale particles do not observed.

## INTRODUCTION

At present, the coatings of DNG/AM (dispersed nanograins in amorphous matrix) type are widespread for creation of materials with special properties [1]. The advantage of these coatings is the presence of a protective surface layer with a high mechanical, tribological and other properties such as high hardness, low friction, wear resistance and high thermal stability [2].

Coatings based on amorphous carbon and nanocrystalline particles are the most promising in terms of materials creation with high antifriction properties. These particles increase the strength of amorphous matrix. Amorphous carbon is a solid lubricant at the interaction of pairs of friction.

The solid solution doping of the amorphous carbon matrix of DNG/AM coatings by the elements such as Ti, Cr, Al, Si can significantly reduce internal stresses due to changes in bonds type of amorphous carbon [3].

At present paper the microstructure, mechanical and tribological properties, thermal stability, and elastically stressed state of nanocrystalline particles in Ti-C-Ni-Cr и Ti-C-Ni-Cr-Al-Si coatings have been investigated.

## EXPERIMENTAL PROCEDURE

The coatings based on amorphous carbon and the nanosized particles were synthesized in the plasma magnetron-arc facility “Legend” [4] with three graphite cathodes (C<sub>1</sub>, C<sub>2</sub>, C<sub>3</sub>) and one composite titanium-carbide cathode using nichrome as a binder. To form a Ti-C-Ni-Cr-Al-Si coating, one of the graphite cathodes was replaced by an AlCrSi cathode. Deposition parameters are given in Table 1. The substrates were made from VT1-0 titanium alloy.

**TABLE 1.** Modes of Ti-C-Ni-Cr и Ti-C-Ni-Cr-Al-Si coatings synthesis

Coating		P, kW			$U_s, V$	$T, ^\circ C$	$t, min$	$P_{Ar+N_2}, Torr$
Ti-C-Ni-Cr	TiCNiCr	$C_1$	$C_2$	$C_3$	50	450	60	$4 \times 10^{-3}$
	1.2–1.3	0.9	0.9	0.9				
Ti-C-Ni-Cr-Al-Si	TiCNiCr	AlCrSi	$C_1$	$C_2$	50	450	60	$4 \times 10^{-3}$
	1.2–1.3	0.4	0.9	0.9				

Investigation of samples by transmission electron microscopy (TEM) was performed on microscope Philips CM-12 at an accelerating voltage of 120 kV and on JEOL 2100 (accelerating voltage 200 kV). Thin foils were prepared from cross section by a focused ion beam on Quanta 200 3D equipment.

Microhardness of coatings was measured by the Vickers method using a special attachment to a Neophot-21 optical microscope. Tempering at temperatures up to 900°C under a high vacuum of  $2 \times 10^{-5}$  Torr have been made. Tribological tests have been carried out at room temperature by a high-temperature tribometer in a ball-on-disk mode with a normal load of 2 N on the spherical indenter.

## RESULTS AND DISCUSSION

Investigation of the Ti-C-Ni-Cr and Ti-C-Ni-Cr-Al-Si coatings by transmission electron microscopy reveals the presence of TiC and NiCr nanocrystalline particles, uniformly distributed in the amorphous phase. The sizes of TiC particles are 2–10 nm. NiCr particles are the solid solution of chromium (up to 20 at %) in nickel (Fig. 1b). The microstructure of the Ti-C-Ni-Cr and Ti-C-Ni-Cr-Al-Si coatings is qualitatively similar. However, the content of carbon in the Ti-C-Ni-Cr-Al-Si coating is reduced in several times due to replacing of the carbon cathode by the AlCrSi composite cathode. In this coating the elements Al and Si are in solid solution in the amorphous phase.

The study of cross-sections of these coatings showed an unhomogenous distribution of nanocrystalline particles from substrate to surface. Near the substrate relatively large (up to 30 nm) NiCr particles are found. Beyond from the substrate the coatings are presented by uniformly distributed particles with the sizes up to 10 nm.

Investigation of the microstructure of Ti-C-Ni-Cr and Ti-C-Ni-Cr-Al-Si coatings after tempering indicates that it is preserved up to  $T = 900^\circ C$ . Changes of the particle sizes of nanocrystalline phases do not occur.

Tribological tests demonstrate that the values of friction coefficient for Ti-C-Ni-Cr coatings are  $\mu \approx 0.14–0.16$  in the initial state compared to that characteristic of the titanium alloy ( $\mu \approx 0.5–0.6$ ) and remain during tempering up to 700°C. Values of the friction coefficient for Ti-C-Ni-Cr-Al-Si coatings after tempering at  $T = 900^\circ C$  do not change as compared with the initial values ( $\mu \approx 0.34$ ). At the same time there is a significant change in the character of friction coefficient dependence from the distance traveled by the indenter. It may be caused by the precipitation of new phases increasing the coefficient of friction.

Investigations of mechanical properties of the titanium alloy samples with Ti-C-Ni-Cr coating (thickness is 2.8  $\mu m$ ) showed that the microhardness value of the «coating + substrate» composition (Fig. 1a) maintains up to  $T = 900^\circ C$ . Moreover, some increase in the hardness from  $\approx 14$  GPa in the initial state to  $\approx 18$  GPa after annealing is observed (Table 2). In our opinion it is caused by the formation of oxide phases on the coating surface. The microhardness values of coatings under study are in  $\approx 5–7$  times higher than that of titanium alloy (2 GPa).

**TABLE 2.** The microhardness  $H_\mu$  of the studied coatings before and after the tempering

Coating	Load, g	$H_\mu$ before tempering, GPa	$H_\mu$ after tempering 900°C, GPa
Ti-C-Ni-Cr	20	$13.9 \pm 0.9$	$18.3 \pm 0.9$
Ti-C-Ni-Cr-Al-Si		$10.7 \pm 1.5$	$9.4 \pm 1.1$

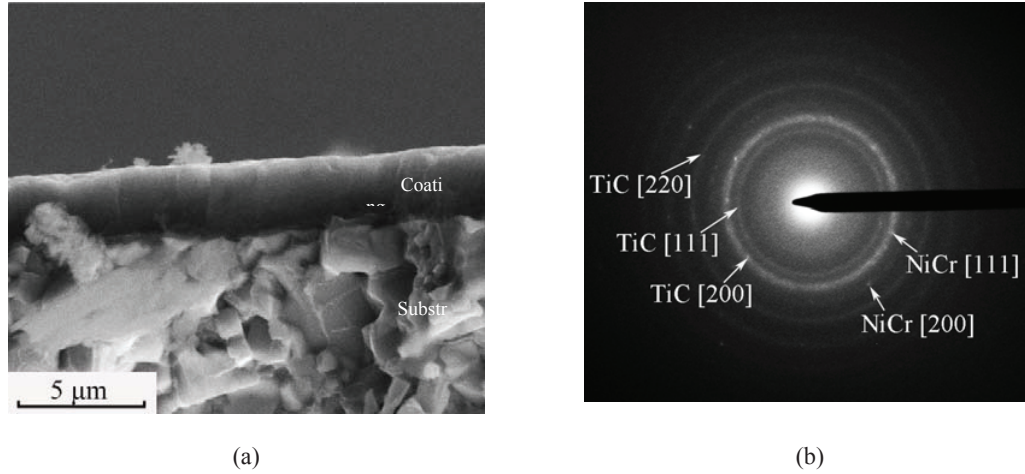


**FIGURE 1.** Cross-section image of the Ti-C-Ni-Cr coating formed by SEM (a) and the microdiffraction pattern (b)

The Ti-C-Ni-Cr-Al-Si coatings (thickness is 2.6  $\mu\text{m}$ ) on the titanium alloy samples already in the initial state have a somewhat lower hardness (10.7 GPa). Tempering at 900°C of these coatings causes a reduction of microhardness values up to  $\approx 9.4$  GPa.

In this work the features of elastically stressed state of TiC particles in the cross sections of Ti-Ni-Cr-C and Ti-C-Ni-Cr-Al-Si coatings after deposition and tempering using the special dark-field TEM analysis were investigated. It includes a step-by-step tilt of foil in goniometer. In these techniques displacement of extinction contour at tilt of foil in goniometer is associated with the  $\chi_{21}$  component of crystal lattice curvature tensor. This component corresponding to the change in orientation of the crystallographic planes that are parallel to the plane of the foil [5]:

$$\chi_{21} = \frac{\Delta\varphi \sin \beta}{\Delta r}, \quad (1)$$

$\Delta r$ —displacement of contour at a tilt of the foil in goniometer,  $\Delta\varphi$ —angle of the foil tilt,  $\beta$ —angle between operative reflection vector and direction of the tilt axis projection.

In the Fig. 2 an example of the dark-field analysis of Ti-C-Ni-Cr coating in the initial state during tilt (by 0.5°) in TiC reflection  $g = [111]$  is presented. At the tilt of goniometer on 1.5° the extinction contour in the particle with diameter of  $\approx 10$  nm moves from the left to the right side. According to (1) the component  $\chi_{21}$  is  $\approx 75^\circ/\mu\text{m}$ . According to [5] the local internal stresses value  $\sigma_{\text{loc}}$  in the particle is:

$$\sigma_{\text{loc}} = \frac{E\chi_{ij}\Delta h}{2}, \quad (2)$$

$E$ —Young's modulus,  $\chi_{ij}$ —component of crystal lattice curvature tensor,  $\Delta h$ —zone sizes of a lattice high curvature.

Estimated value is  $\approx E/150$ . The obtained values of local internal stresses is at least several times less than analogous values for particles in the superhard coatings based on titanium nitride [5]. It corresponds with our earlier results about the absence of high local internal stresses in nanoscale particles of the Ti-C-Ni-Cr coating [6].

The angular range of the diffraction peak exitance in the TiC particle of Ti-C-Ni-Cr coating after tempering at  $T = 900^\circ\text{C}$  is  $\approx 1.75^\circ$ . This value is comparable with a broadening of the diffraction peak (1.5°) due to the small (10 nm) particle sizes. At the same time, displacement of the extinction contour during tilt does not observed. It is proposed that these effects are related to the absence of high values of crystal lattice curvature in TiC nanoscale particles. During tempering the value of local internal stresses in the particles is decreased. The structural state of nanoscale particles in the Ti-C-Ni-Cr-Al-Si coating is completely analogous to the state considered above.

The low values of the curvature tensor components correspond to the low internal stresses in nanoscale TiC particles. It is a significant difference between these particles and TiN nanoscale particles in the superhard coatings in which the local internal stresses can achieve the theoretical strength of the crystal [5]. In our opinion the difference in the structural state of the particles can be caused by the less constrained conditions of particles in the amorphous carbon as compared with the superhard coatings.

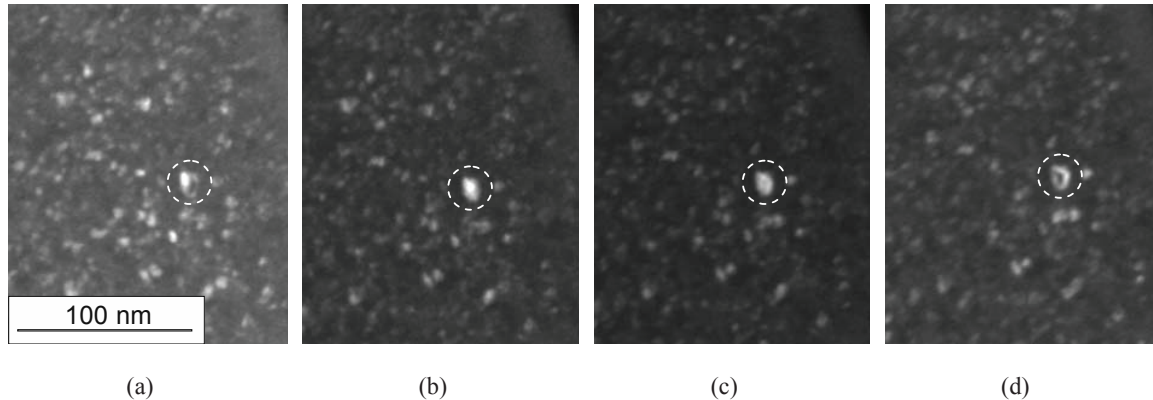


**FIGURE 2.** Dark-field electron-microscope images of the Ti-C-Ni-Cr coating in the initial state, received with tilt in the  $g = [111]$  TiC. Tilt angles: 2.6° (a), 3.2° (b), 3.6° (c), 4.1° (d). Angle between projection of goniometer axis and acting reflection  $\beta \sim 30^\circ$ ,  $\sin\beta = 0.5$

## CONCLUSION

Multielement nanocomposite Ti-C-Ni-Cr and Ti-C-Ni-Cr-Al-Si coatings, having a sufficiently high (11–18 GPa) hardness, low ( $\mu < 0.2$ ) the coefficient of friction and high thermal stability of the microstructure and properties up to 700°C were obtained. These properties are caused by the structure of amorphous carbon and nanosized TiC and NiCr particles. It demonstrates the possibility of applying of the considered coatings on the manufactures of titanium alloys to hardening and reduction of the friction coefficient.

The microstructure of coatings is represented by the amorphous matrix with dissolved Al, Si, Cr, Ni metal elements and nanosized particles of crystalline phases (TiC and NiCr). A high local internal stresses in the nanoscale particles by the dark-field TEM analysis do not observed. It is a fundamental difference between these particles and nanosized particles in a superhard coatings. This difference is caused by the ability of amorphous carbon to the relaxation of high internal stresses.

## ACKNOWLEDGMENTS

This work has been performed with a support of RFBR (Grant No. 13-02-98020 r\_sibir\_a) (experimental work) and Tomsk State University Competitiveness Improvement Program (structural investigations).

## REFERENCES

1. J. Musil, *Surf. Coat. Tech.* **207**, 50–65 (2012).
2. D. G. Teer, *Wear* **251**, 1068–1074 (2001).
3. J. Musil, *Physical and Mechanical Properties of Hard Nanocomposite Films Prepared by Reactive Magnetron Sputtering* (Springer, 2006), pp. 407–463.
4. D. P. Borisov, K. N. Detistov, A. A. Zenin, A. D. Korotaev, V. M. Kuznetsov, A. N. Tyumentsev, and E. V. Chulkov, *Russ. Phys. J.* **54**(9-2), 19–26 (2011).
5. A. D. Korotaev, D. P. Borisov, V. Yu. Moshkov, S. V. Ovchinnikov, A. N. Tyumentsev, and G. A. Pribytkov, *Phys. Mesomech.* **16**(1), 73–83 (2013).
6. A. V. Andreev, I. Yu. Litovchenko, A. D. Korotaev, D.P. Borisov, Features of Structure-Phase State of Multielement Nanocomposite Coatings Based on Amorphous Carbon, in *Physical Mesomechanics of Multilevel Systems-2014*, AIP Conference Proceedings 1623, edited by V. E. Panin, et al. (American Institute of Physics, Melville, NY, 2014), pp. 11–14.